157
3/1/79

DR. 2292

ORNL/TM-6421

# Beam Profiles from Multiple Aperture Sources

J. H. Whealton



OAK RIDGE NATIONAL LABORATORY
OPERATED BY UNION CARBIDE CORPORATION · FOR THE DEPARTMENT OF ENERGY

# DISCLAIMER

Printed in the United States of America. Available from
National Technical Information Service
U.S. Department of Commerce
5285 Port Royal Road, Springfield, Virginia 22161
Price: Printed Copy $4.00; Microfiche $3.00

ORNL/TM-6421
Dist. Category UC-20 a

Contract No. W-7405-eng-26

FUSION ENERGY DIVISION

# BEAM PROFILES FROM MULTIPLE APERTURE SOURCES

J. H. Whealton

Date Published: February, 1979



**NOTICE** This document contains information of a preliminary nature. It is subject to revision or correction and therefore does not represent a final report.

Prepared by the
OAK RIDGE NATIONAL LABORATORY
Oak Ridge, Tennessee 37830
operated by
UNION CARBIDE CORPORATION
for the
DEPARTMENT OF ENERGY

THIS PAGE

WAS INTENTIONALLY

LEFT BLANK

ABSTRACT

Using a rapidly convergent approximation scheme, formulas are given for beam intensity profiles everywhere. In first approximation, formulas are found for multiple aperture sources, such as a TFTR design, and integrated power for rectangular plates downstream for Gaussian beamlets. This analysis is duplicated for Lorentzian beamlets which should provide a probable upper bound for off-axis loading as Gaussian beamlets provide a probable lower bound. Formulas for beam intensity profiles are found everywhere. In first approximation, formulas are found for downstream intensity of multiple sources and integrated power for rectangular plates.

Previous analysis[1] includes formulas for the beam power intensity for Gaussian beamlets at (a) the focal plane, (b) on the beam axis, and (c) very near the beam axis. By considering a rapidly convergent approximation scheme these results are extended to give beam power intensities everywhere and, in first approximation, beam intensities everywhere for multiple, but closely spaced, sources. Total beam power deposited on a rectangular plate is also given.

Consider the coordinate system and approximation scheme shown in Fig. 1 where the circular source is approximated by a square one. The intensity at a point $\zeta$, $\eta$, $\xi$ from an element in the source is

$$di(\zeta,\eta,\xi) = \frac{1}{\pi(\xi\theta)^2} \exp\left[-\frac{(\zeta^2+\eta^2)}{(\xi\theta)^2}\right] d\zeta d\eta, \tag{1}$$

and the intensity at a point $\zeta$, $\eta$, $\xi$ from the entire source, in first approximation, is

$$i_1(\zeta,\eta,\xi) = \frac{1}{\pi(\xi\theta)^2} \int_{-1/2}^{+1/2} d\zeta' \int_{-1/2}^{+1/2} d\eta' \exp\left[-\frac{(\zeta'-\zeta)^2+(\eta'-\eta)^2}{(\xi\theta)^2}\right]. \tag{2}$$

Integration gives the result:

$$i_1(\zeta,\eta,\xi) = \frac{1}{4}\left[\operatorname{erf}\left(\frac{1-2\zeta}{2\xi\theta}\right) + \operatorname{erf}\left(\frac{1+2\zeta}{2\xi\theta}\right)\right] \times \left[\operatorname{erf}\left(\frac{1-2\eta}{2\xi\theta}\right) + \operatorname{erf}\left(\frac{1+2\eta}{2\xi\theta}\right)\right]. \tag{3}$$

If focusing is considered as in the above figure, i is divided by $(1-\xi/\lambda)^2$ and the limits of integration in Eq. (2) are multiplied by $1-\xi/\lambda$ giving the result, in first approximation,

$$i_1(\zeta,\eta,\xi) = \frac{\lambda^2}{4(\lambda - \xi)^2} \left\{ \mathrm{erf}\left[\frac{\lambda(1 - 2\zeta) - \xi}{2\lambda\xi\theta}\right] + \mathrm{erf}\left[\frac{\lambda(1 + 2\zeta) - \xi}{2\lambda\xi\theta}\right] \right\} \times \left\{ \mathrm{erf}\left[\frac{\lambda(1 - 2\eta) - \xi}{2\lambda\xi\theta}\right] + \mathrm{erf}\left[\frac{\lambda(1 + 2\eta) - \xi}{2\lambda\xi\theta}\right] \right\}, \tag{4}$$

which at the focal plane, using the asymptotic properties of the error function, becomes in any approximation

$$i(\zeta,\eta,\lambda) = \frac{1}{\pi(\xi\theta)^2} \exp\left[ - \frac{\zeta^2 + \eta^2}{(\xi\theta)^2} \right], \tag{5}$$

in agreement with previous analysis.[1] On the axis the intensity becomes in first approximation

$$i_1(0,0,\xi) = \frac{\lambda^2}{(\lambda - \xi)^2} \left[ \mathrm{erf}\left( \frac{\lambda - \xi}{2\lambda\xi\theta} \right) \right]^2, \tag{6}$$

in contrast with the exact results in the previous analysis,

$$i(0,0,\xi) = \frac{\lambda^2}{(\lambda - \xi)^2} \left\{ 1 - \exp\left[ - \frac{(\lambda - \xi)^2}{\pi(\lambda\xi\theta)^2} \right] \right\}. \tag{7}$$

In second approximation, as shown in Fig. 1, two square sources are considered at 45° to each other. The result it

$$i_2(\zeta,\eta,\xi) = \frac{1}{2} i_1(\zeta,\eta,\xi) + \frac{1}{2} i_1\left( \frac{\zeta + \eta}{\sqrt{2}}, \frac{\eta - \zeta}{\sqrt{2}}, \xi \right), \tag{8}$$

and so on for the $n^{th}$ approximation,

$$i_n(\zeta,\eta,\xi) = \frac{1}{n} \sum_{m=0}^{n-1} i_1\left( \zeta \cos\frac{m\pi}{2n} + \eta \sin\frac{m\pi}{2n}, \eta \cos\frac{m\pi}{2n} - \zeta \sin\frac{m\pi}{2n}, \right) \tag{9}$$

For multiple sources (e.g., three) the total beam intensity at a point is in first approximation:

$$i_{III}(\zeta,\eta,\xi) = i_1(\zeta,\eta,\xi) + i_1[\zeta,\eta - \alpha(\lambda - \xi),\xi] + i_1[\zeta,\eta + \alpha(\lambda - \xi),\xi], \tag{10}$$

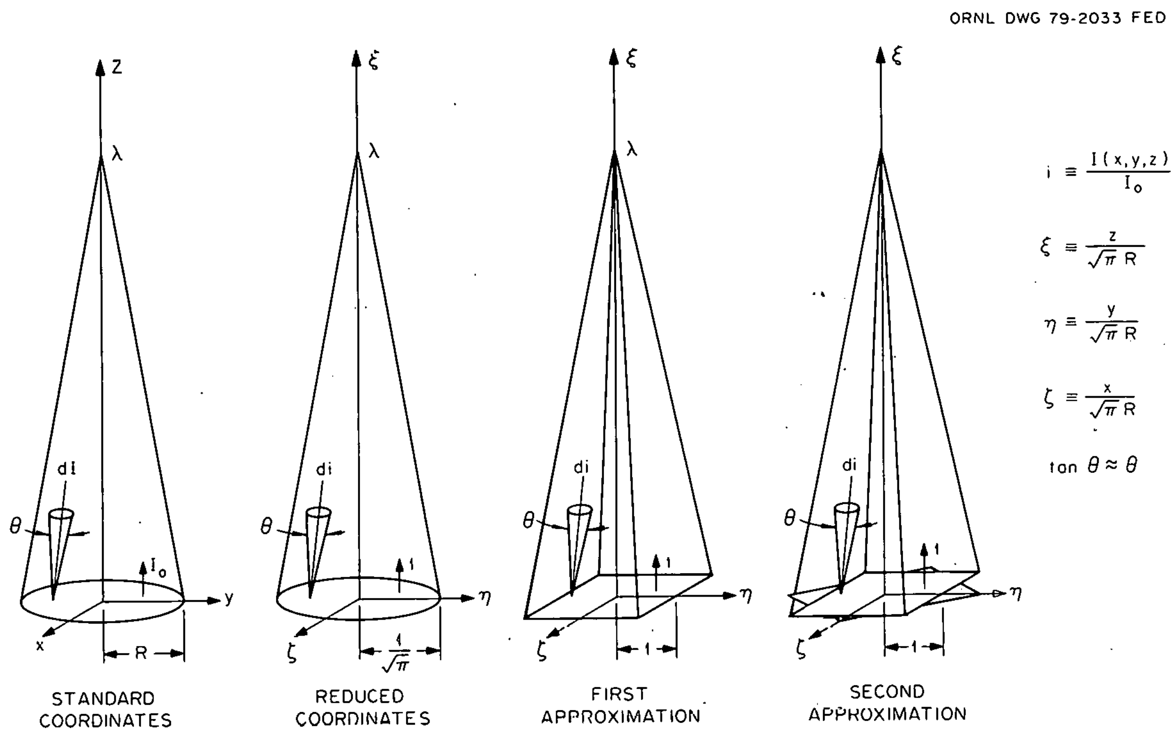


Fig. 1. The square peg in a round hole approximation scheme.

where the configuration of the three sources is shown in Fig. 2.

Finally the integrated power is computed from a single source in first approximation over the hatched area in Fig. 3, which is

$$\int_{\beta}^{\infty} d\zeta \int_{-\gamma}^{+\gamma} d\eta \; i_1(\zeta,\eta,\xi) = \frac{\lambda^2}{2(\lambda - \xi)^2} \, g(\gamma)\; g(-\beta) \tag{11}$$

where

$$g(\gamma) = \xi\theta\Bigg(\left[\frac{\lambda(1 + 2\gamma) - \zeta}{2\lambda\xi\theta}\right] \operatorname{erf}\left[\frac{\lambda(1 + 2\gamma) - \xi}{2\lambda\xi\theta}\right] - \left[\frac{\lambda(1 - 2\gamma) - \xi}{2\lambda\xi\theta}\right] \operatorname{erf}\left[\frac{\lambda(1 - 2\gamma) - \xi}{2\lambda\xi\theta}\right] - \frac{1}{\sqrt{\pi}} \exp\left\{-\left[\frac{\lambda(1 + 2\gamma) - \xi}{2\lambda\xi\theta}\right]^2\right\} + \frac{1}{\sqrt{\pi}} \exp\left\{-\left[\frac{\lambda(1 - 2\gamma) - \xi}{2\lambda\zeta\theta}\right]^2\right\}\Bigg), \tag{12}$$

the extension to three sources being obvious.

The inaccuracy of the first approximation is clearly very small near the focal plane and larger outside.

Perhaps it is worthwhile to note that the analysis in first approximation is directly applicable to the Berkeley source providing that the tensoral divergence angle is included by starting from

$$di(\zeta,\eta,\xi) = \frac{1}{\pi\theta_{\|}\theta_{\perp}\xi^2} \exp\left[-\left(\frac{\zeta^2}{\theta_{\|}\xi^2} + \frac{\eta^2}{\theta_{\perp}\xi^2}\right)\right] d\eta\, d\zeta \;,$$

instead of Eq. (1).

An assumption in the foregoing is that individual beamlets have a Gaussian profile. Since such a profile has a very rapid off-axis fall-off and since certain beam line designs may depend on wall loading, a Lorentzian beamlet profile is considered. A Lorentzian profile falls off more slowly off-axis as is seen in Fig. 4. The same approximation scheme and analysis as mentioned above is presented below for Lorentzian beamlets.

ORNL DWG 79-2034 FED

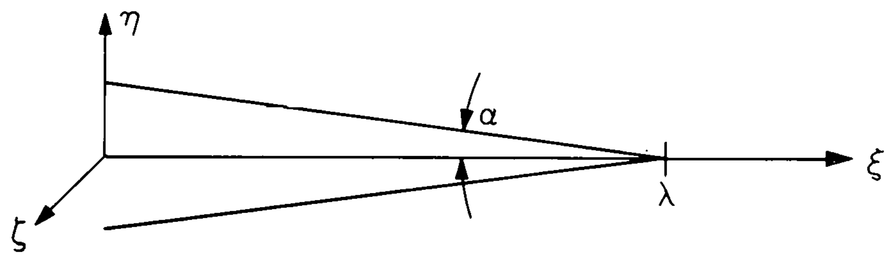


Fig. 2. Three source configuration.

ORNL DWG 79-2035 FED

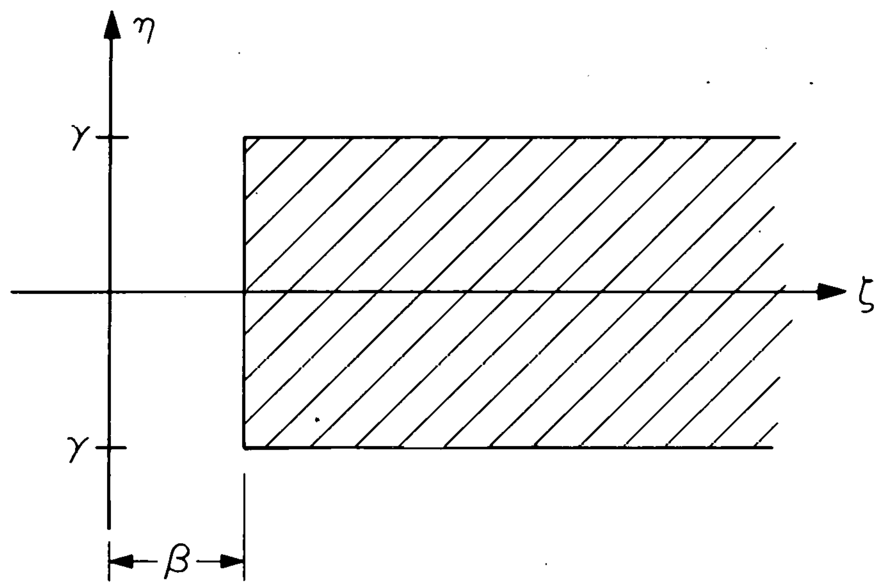


Fig. 3. Region of total power computation.

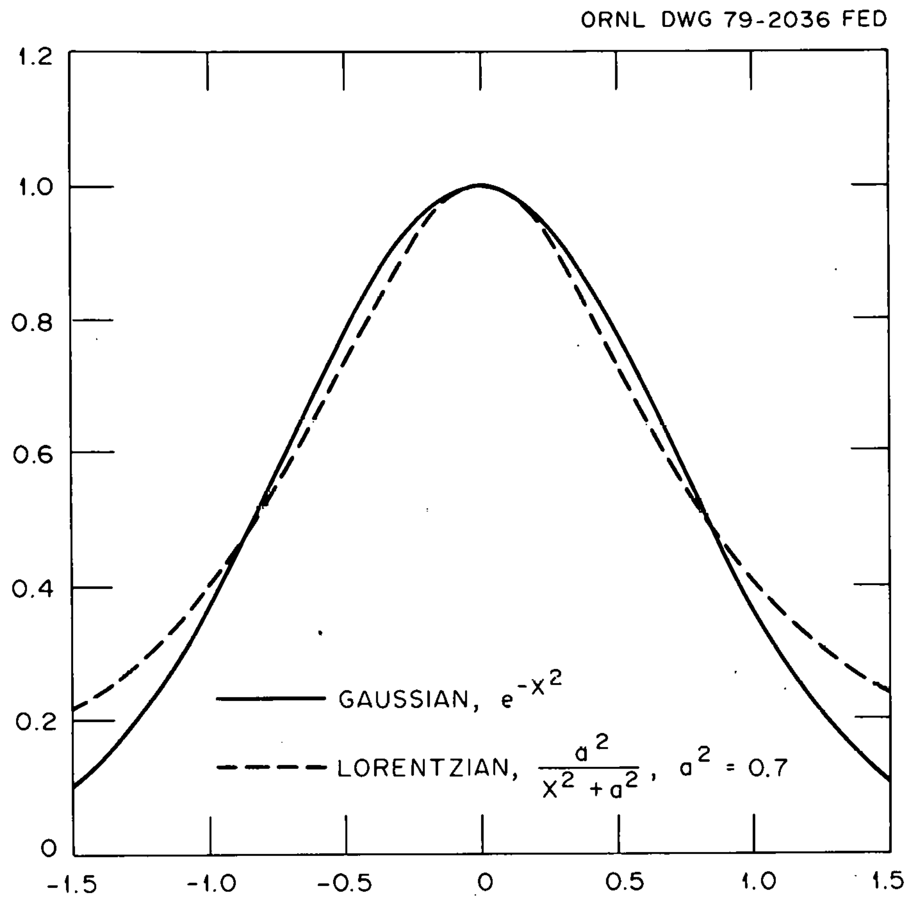


Fig. 4. Comparison of Gaussian and Lorentzian.

Consider the coordinate system and approximation scheme as shown in Fig. 1 where the circular source is approximated by a square one. The intensity at a point $\zeta$, $\eta$, $\xi$ from an element in the source is

$$di(\zeta,\eta,\xi) = \frac{(\xi\theta/\pi)^2}{(\zeta^2 + \xi^2\,\theta^2)(\eta^2 + \xi^2\,\theta^2)}\, d\zeta d\eta \ , \tag{13}$$

where the divergence angle $\theta$ is the half max angle of the Lorentzian distribution along one axis. The beamlet distribution is not quite cylindrically symmetric but this artifact washes out in higher approximations. The intensity at a point $\zeta$, $\eta$, $\xi$ from the entire source, in first approximation, is

$$i_1(\zeta,\eta,\xi) = \left(\frac{\xi\theta}{\pi}\right)^2 \int_{-1/2}^{+1/2} d\zeta' \int_{-1/2}^{+1/2} d\eta' \left[(\zeta' - \zeta)^2 + \xi^2\theta^2\right]^{-1} \times \left[(\eta' - \eta)^2 + \xi^2\theta^2\right]^{-1} . \tag{14}$$

Integration gives the result:

$$i_1(\zeta,\eta,\xi) = \frac{1}{\pi^2}\left[\arctan\left(\frac{1 - 2\zeta}{2\xi\theta}\right) + \arctan\left(\frac{1 + 2\zeta}{2\xi\theta}\right)\right] \times \left[\arctan\left(\frac{1 - 2\eta}{2\xi\theta}\right) + \arctan\left(\frac{1 + 2\eta}{2\xi\theta}\right)\right] . \tag{15}$$

If focusing is considered as in Fig. 1, $i$ is divided by $(1 - \xi\lambda)^2$ and the limits of integration in Eq. (14) are multiplied by $1 - \xi/\lambda$ giving the result

$$i_1(\zeta,\eta,\xi) = \frac{(\lambda/\pi)^2}{(\lambda - \xi)^2}\left\{\arctan\left[\frac{\lambda(1 - 2\zeta) - \xi}{2\lambda\xi\theta}\right] + \arctan\left[\frac{\lambda(1 + 2\zeta) - \xi}{2\eta\xi\theta}\right]\right\} \times \left\{\arctan\left[\frac{\lambda(1 - 2\eta) - \xi}{2\lambda\xi\theta}\right] + \arctan\left[\frac{\lambda(1 + 2\eta) - \xi}{2\lambda\xi\theta}\right]\right\} \tag{16}$$

which at the focal plane using the asymptotic properties of the arc tangent becomes

$$i_1(\zeta,\eta,\lambda) = \frac{(\lambda/\pi)^2}{(\zeta^2 + \lambda^2\theta^2)(\eta^2 + \lambda^2\theta^2)} \quad . \tag{17}$$

On the axis the intensity becomes in first approximation

$$i_1(0,0,\xi) = \frac{4(\lambda/\pi)^2}{(\lambda - \xi)^2} \left[\arctan\left(\frac{\lambda - \xi}{2\lambda\xi\theta}\right)\right]^2 \quad . \tag{18}$$

In second approximation two square sources are considered at 45° to each other, as shown in Fig. 1.

For multiple sources (e.g., three) the total beam intensity at a point is approximately in first approximation by Eq. (10) where the configuration of the three sources is shown in Fig. 2.

Finally the integrated power is computer from a single source in first

$$\int_\beta^\infty d\zeta \int_{-\gamma}^{+\gamma} d\eta \; i_1(\zeta,\eta,\xi) = \frac{2(\lambda/\pi)^2}{(\lambda \quad \xi)^2} \, g(\gamma) \; g(-\beta) \quad , \tag{19}$$

$$\begin{aligned} g(\gamma) = \xi\theta\Bigg(&\left[\frac{\lambda(1 + 2\gamma) - \xi}{2\lambda\xi\theta}\right] \arctan\left[\frac{\lambda(1 + 2\gamma) - \xi}{2\lambda\xi\theta}\right] - \left[\frac{\lambda(1 - 2\gamma) - \xi}{2\lambda\xi\theta}\right] \\ &\times \arctan\left[\frac{\lambda(1 - 2\gamma) - \xi}{2\lambda\xi\theta}\right] \\ &- \frac{1}{2}\log\left\{(2\lambda\xi\theta)^2 + [\lambda(1 + 2\gamma) - \xi]^2\right\} \\ &+ \frac{1}{2}\log\left\{(2\lambda\xi\theta)^2 + [\lambda(1 - 2\gamma) - \xi]^2\right\} \quad , \end{aligned} \tag{20}$$

the extension to three sources being obvious.

The inaccuracy of the first approximation is clearly very small near the focal plane and larger outside.

As with the Gaussian beamlet case, it is worthwhile to note that the analysis in first approximation is directly applicable to the Berkeley source providing that the tensoral divergence angle is included by starting from

$$di(\zeta,\eta,\xi) = \frac{\xi^2\theta_{\parallel}\theta_{\perp}/\pi^2}{(\zeta^2 + \xi^2\theta_{\parallel}^2)(\eta^2 + \xi^2\theta_{\perp}^2)}\, d\eta d\zeta \quad . \tag{24}$$

This analysis was done in April 1976 and partially reported in Nuclear Instruments and Methods 141, 187 (1977). At the time there was little evidence for fatter distributions than Gaussian. However, since that time such evidence has accumulated. In connection with re-ionization loss calculations accounting for direct beam interception, these calculations assume new importance and this report is issued in response to this demand.

## REFERENCE

1. J. Kim (ORNL) private communication (1975).

ORNL/TM-6421
Dist. Category UC-20 a

INTERNAL DISTRIBUTION

1. G. C. Barber
2. C. F. Barnett
3. L. A. Berry
4. C. W. Blue
5. J. D. Callen
6. W. K. Dagenhart
7. R. A. Dandl
8. R. C. Davis
9. C. A. Foster
10. W. L. Gardner
11. H. H. Haselton
12. T. C. Jernigan
13. G. G. Kelley
14. J. Kim
15. M. S. Lubell
16. M. M. Menon
17. H. C. McCurdy
18. S. L. Milora
19. O. B. Morgan
20. N. S. Ponte
21. M. Roberts
22. M. W. Rosenthal
23. P. M. Ryan
24. D. E. Schechter
25. S. W. Schwenterly
26. J. Sheffield
27. D. Steiner
28. W. L. Stirling
29. C. C. Tsai
30-59. J. H. Whealton
60. R. E. Wright
61-62. Central Research Library
63. Document Reference Section
64-65. Laboratory Records
66. Laboratory Records, ORNL-RC
67. ORNL Patent Office
68-69. Fusion Energy Division Library
70. Fusion Energy Division Communications Center

EXTERNAL DISTRIBUTION

71. D. J. Anthony, Energy Systems and Technology Division, General Electric Company, 1 River Road, Bldg. 23, Room 2, Schenectady, NY 12345
72. C. Baker, Argonne National Laboratory, 9700 South Cass Avenue, Argonne, IL 60439
73. J. W. Beal, General Atomic Company, P.O. Box 608, San Diego, CA 92112
74. J. F. Clarke, Office of Fusion Energy (ETM), U.S. Department of Energy, Washington, DC 20545
75. F. E. Coffman, Office of Fusion Energy (ETM), U.S. Department of Energy, Washington, DC 20545
76. R. W. Conn, Department of Nuclear Engineering, University of Wisconsin, Madison, WI 53706
77. S. O. Dean, Office of Fusion Energy (ETM), U.S. Department of Energy, Washington, DC 20545
78. H. P. Eubank, Plasma Physics Laboratory, Princeton University, P.O. Box 451, Princeton, NJ 08540
79. T. K. Fowler, Lawrence Livermore Laboratory, University of California, P.O. Box 808, Livermore, CA 94550
80. H. K. Forsen, Exxon Nuclear Company, 2955 George Washington Way, Richland, WA 99352
81. H. P. Furth, Plasma Physics Laboratory, Princeton University, P.O. Box 451, Princeton, NJ 08540

82. R. W. Gould, Electrical Engineering and Physics Department, Bldg. 116-81, California Institute of Technology, Pasadena, CA 91109
83. R. L. Hirsch, Exxon Research and Engineering, P.O. Box 101, Florham Park, NJ 07932
84. Ray Huse, Chairman, EPRI Fusion Program Committee, Public Service Electric and Gas Company, 80 Park Place, Newark, NJ 07101
85. E. E. Kintner, Office of Fusion Energy (ETM), U.S. Department of Energy, Washington, DC 20545
86. S. Matsuda, Japan Atomic Energy Research Institute, Tokai, Ibaraki, Japan
87. Director, Max Planck Instituut für Plasmaphysik, Garching bei München, Federal Republic of Germany
88. G. H. Miley, Nuclear Engineering Program, University of Illinois, Urbana, IL 61801
89. T. Ohkawa, General Atomic Company, P.O. Box 608, San Diego, CA 92112
90. R. V. Pyle, Lawrence Berkeley Laboratory, University of California, Berkeley, CA 94120
91. D. J. Rose, Massachusetts Institute of Technology, James Forrestal Campus, Cambridge, MA 02139
92. N. N. Semasko, Kurchatov Atomic Energy Institute, Moscow, U.S.S.R.
93. T. Sluyters, Brookhaven National Laboratory, Upton, Long Island, NY 11973
94. H. S. Staten, Office of Fusion Energy (ETM), U.S. Department of Energy, Washington, DC 20545
95. L. D. Stewart, Plasma Physics Laboratory, Princeton University, P.O. Box 451, Princeton, NJ 08540
96. E. Thompson, Culham Laboratory, Abingdon, Oxfordshire, United Kingdom
97. P. Raimbault, Centre d'Etudes Nucleairs, B.P. No. 6, Fontenay-aux-Roses, France
98. J. M. Williams, Office of Fusion Energy (ETM), U.S. Department of Energy, Washington, DC 20545
99. J. T. Woo, Massachusetts Institute of Technology, James Forrestal Campus, Cambridge, MA 02139
100. Office of Assistant Manager, Energy Research and Development, Department of Energy, Oak Ridge Operations Office, Oak Ridge, TN 37830

101-253. Given distribution as shown in TID-4500, Magnetic Fusion Energy (Distribution Category UC-20 a, Plasma Systems)